bioRxiv preprint doi: https://doi.org/10.1101/491811; this version posted December 11, 2018. The copyright holder for this preprint (which was not certified by peer review) is the author/funder, who has granted bioRxiv a license to display the preprint in perpetuity. It is made available under aCC-BY-NC-ND 4.0 International license.

Cell type-specific regulation of nutrient absorption, metabolism and transfer in arbuscular mycorrhizal fungi

Hiromu Kameoka[1,a]*, Taro Maeda[1], Nao Okuma[2], Masayoshi Kawaguchi[1,2]*

[1]Division of Symbiotic Systems, National Institute for Basic Biology, 38 Nishigonaka, Myodaiji, Okazaki, Aichi 444-8585, Japan.

[2]The Graduate University for Advanced Studies, 38 Nishigonaka, Myodaiji, Okazaki, Aichi 444-8585, Japan.

[a]Present address: Graduate School of Life and Environmental Sciences, Osaka Prefecture University, 1-1 Gakuen-cho, Naka-ku, Sakai, Osaka 599-8531, Japan

***Corresponding authors:**

Hiromu Kameoka

Tel: +81-72-254-9472; Email address: thk31601@osakafu-u.ac.jp

Masayoshi Kawaguchi

Tel: +81- 564-55-7564; Email address: masayosi@nibb.ac.jp

Keywords: Arbuscular mycorrhizal fungi, transcriptome, nutrient absorption, metabolism, nutrient transfer

bioRxiv preprint doi: https://doi.org/10.1101/491811; this version posted December 11, 2018. The copyright holder for this preprint (which was not certified by peer review) is the author/funder, who has granted bioRxiv a license to display the preprint in perpetuity. It is made available under aCC-BY-NC-ND 4.0 International license.

Abstract

Arbuscular mycorrhizal fungi (AMF) establish symbiotic relationships with most land plants, mainly for the purpose of nutrient exchange. Many studies have revealed the regulation of absorption, metabolism, and transfer of nutrients in AMF and the genes involved in these processes. However, the developmental regulation of the genes associated with cell differentiation are not well understood. Here, we demonstrate the cell type-specific transcriptome of the model AMF species, *Rhizophagus irregularis*. We performed an ultra-low input RNA-seq analysis, SMART-seq2, comparing five cell types in extraradical structures. In addition, we reanalyzed the recently reported RNA-seq data comparing intraradical hyphae and arbuscules. Our analyses captured the distinct features of each cell type and revealed the cell type-specific expression patterns of genes related to absorption, metabolism, and transfer of nutrients. These findings provide a comprehensive dataset to further our understanding of the transcriptional dynamics of fungal nutrition in this symbiotic system.

bioRxiv preprint doi: https://doi.org/10.1101/491811; this version posted December 11, 2018. The copyright holder for this preprint (which was not certified by peer review) is the author/funder, who has granted bioRxiv a license to display the preprint in perpetuity. It is made available under aCC-BY-NC-ND 4.0 International license.

Introduction

Arbuscular mycorrhizal fungi (AMF) establish symbiotic relationships with most terrestrial plants (Brundrett and Tedersoo, 2018). The central function of these relationships is nutrient exchange, in which AMF supply plants with mineral nutrients and water, in exchange for carbon sources (Roth and Paszkowski, 2017). Through this trade, AMF play important roles in terrestrial ecosystems (van der Heijden et al., 2008, 1998), and contribute to an increase in agricultural productivity (Igiehon and Babalola, 2017). Therefore, it is important to understand the regulation of absorption, metabolism and transfer of nutrients associated with the symbiotic state of AMF.

Phosphate and nitrogen are important nutrients absorbed by AMF from soil and then transferred to host plants (Govindarajulu et al., 2005; Pearson and Jakobsen, 1993). AMF absorb inorganic phosphate (Pi) from soil using two types of phosphate importer, the H^+-Pi symporter and the Na^+-Pi symporter (Harrison and van Buuren, 1995; Maldonado-Mendoza et al., 2001; Tisserant et al., 2012; Walder et al., 2016). AMF also utilize organic phosphate by secreting acid phosphatase (Sato et al., 2015). Most of the Pi absorbed by the extraradical mycelium (ERM) is transformed into polyphosphate, presumably in the tonoplast by the vacuolar transporter chaperone (VTC) complex, and then transported to the intraradical mycelium (IRM) through vacuoles (Hijikata et al., 2010; Kuga et al., 2008; Tani et al., 2009; Viereck et al., 2004). Polyphosphate is probably degraded to monophosphate by polyphosphatase and subsequently released from AMF (Capaccio and Callow, 1982). Although the mechanism by which AMF release Pi is largely unknown, SYG1 orthologs are strong candidates for the Pi exporter (Azevedo and Saiardi, 2017; Ezawa and Saito, 2018). In the case of nitrogen, AMF absorb NO_3^- and NH_4^+, and transform them into arginine in the ERM. Arginine is transported into the IRM through

bioRxiv preprint doi: https://doi.org/10.1101/491811; this version posted December 11, 2018. The copyright holder for this preprint (which was not certified by peer review) is the author/funder, who has granted bioRxiv a license to display the preprint in perpetuity. It is made available under aCC-BY-NC-ND 4.0 International license.

61 vacuoles and degraded into NH_4^+ before being transferred to host plants (Cruz et al., 2007;
62 Govindarajulu et al., 2005; Jin et al., 2005; Tian et al., 2010). Many genes which encode
63 transporters and enzymes involved in these processes have been identified (Calabrese et
64 al., 2016; López-Pedrosa et al., 2006; Pérez-Tienda et al., 2011; Tian et al., 2010).

65 Conversely, AMF strongly depend on plants as their source of carbon (Bago et al.,
66 2000; Roth and Paszkowski, 2017), although they have the ability to absorb acetate and
67 monosaccharide on the ERM and germinating spores (Bago et al., 2000; Helber et al.,
68 2011; Pfeffer et al., 1999). AMF acquire monosaccharides by using monosaccharide
69 transporters (MSTs) (Ait Lahmidi et al., 2016; Helber et al., 2011; Lammers et al., 2001),
70 and catabolize them via the glycolytic pathway and TCA cycle (Macdonald and Lewis,
71 1978; Saito, 1995). On the other hand, they synthesize trehalose and glycogen to maintain
72 monosaccharide concentrations inside the cells and to transport carbon to the ERM (Bago
73 et al., 2003, 2000; Shachar-Hill et al., 1995). In addition, recent studies have revealed
74 direct lipid transfer from plants to AMF (Jiang et al., 2017; Keymer et al., 2017;
75 Luginbuehl et al., 2017). AMF can elongate and desaturate fatty acids but not synthesize
76 them (Trépanier et al., 2005), because they lack cytosolic fatty acid biosynthesis genes
77 (Kobayashi et al., 2018; Maeda et al., 2018; Sun et al., 2018; Tang et al., 2016; Wewer et
78 al., 2014), indicating that all fatty acids in AMF are plant-derived. The molecular form of
79 transferred lipid is still unknown, but the predicted catalytic properties of the plant
80 enzymes required just before lipid transfer imply that *sn*-2-palmitoylglycerol is a strong
81 candidate (Brands et al., 2018; Bravo et al., 2017, 2016; Jiang et al., 2017; Keymer et al.,
82 2017; Luginbuehl et al., 2017). AMF produce ATP and synthesize saccharides from fatty
83 acids via the β-oxidation pathway, the glyoxylate cycle, and the gluconeogenesis pathway
84 (Bago et al., 1999; Lammers et al., 2001; Pfeffer et al., 1999; Wewer et al., 2014).

bioRxiv preprint doi: https://doi.org/10.1101/491811; this version posted December 11, 2018. The copyright holder for this preprint (which was not certified by peer review) is the author/funder, who has granted bioRxiv a license to display the preprint in perpetuity. It is made available under aCC-BY-NC-ND 4.0 International license.

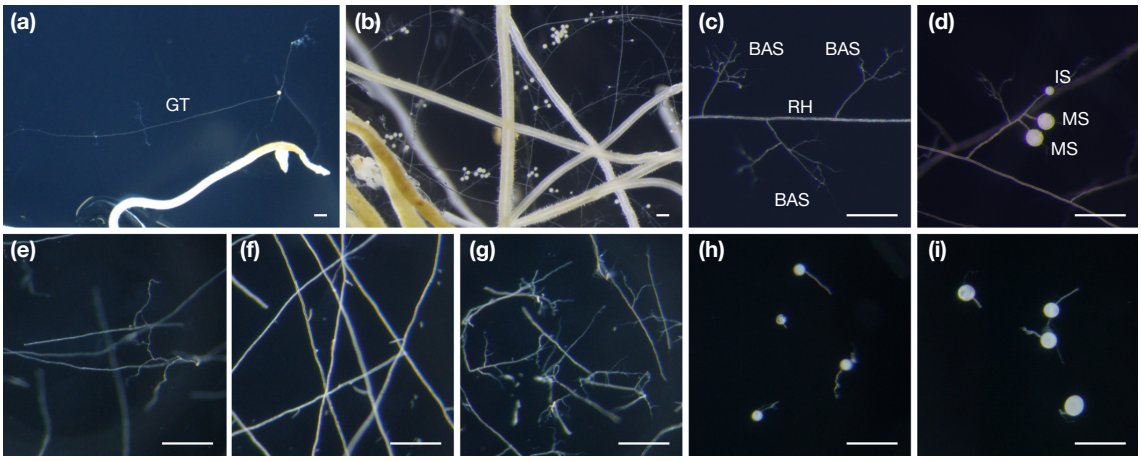

Fig. 1 Cell types of extraradical structures. (a) 1-week-cultured *R. irregularis* in the pre-symbiotic stage. **(b–d)** 6-week-cultured *R. irregularis* in the symbiotic stage; global view **(b)**, runner hyphae and branched absorbing structures **(c)**, and immature and mature spores **(d)**. **(e–i)** Samples for RNA-seq analysis; germ tubes **(e)**, runner hyphae **(f)**, branched absorbing structures **(g)**, immature spores **(h)**, and mature spores **(i)**. Bar = 200 μm. GT, germ tubes; RH, runner hyphae; BAS, branched absorbing structures; IS, immature spores; MS, mature spores.

As described above, many studies to date have shown the regulation of absorption, metabolism and transfer of nutrients in AMF and the genes involved in these processes. Some of these studies investigated the differences between developmental stages, such as between germinating spores, the IRM, and the ERM. However, the differences between the cell types comprising each developmental stage are not well understood. In pre-symbiotic stages, AMF grow curved, thin hyphae called germ tubes (GT) from spores (Fig. 1a). When the GT attach to host roots, the AMF start to grow intraradical hyphae (IRH) and develop arbuscules (ARB). As the plant phosphate transporters, ammonium transporters, and lipid metabolism enzymes required for arbuscular mycorrhizal (AM) symbiosis are specifically expressed in arbuscule-containing cells, it is thought that the transport of phosphorus, nitrogen and lipids occurs in arbuscules (Bravo et al., 2017; Breuillin-Sessoms et al., 2015; Harrison et al., 2002; Keymer et al., 2017; Kobae et al.,

bioRxiv preprint doi: https://doi.org/10.1101/491811; this version posted December 11, 2018. The copyright holder for this preprint (which was not certified by peer review) is the author/funder, who has granted bioRxiv a license to display the preprint in perpetuity. It is made available under aCC-BY-NC-ND 4.0 International license.

2010; Luginbuehl et al., 2017; Yang et al., 2012). The spatial expression patterns of the AMF genes required for nutrient transfer and metabolism, however, have not been well examined. Moreover, the site of saccharide transport is still under debate (Fitter, 2006; Helber et al., 2011). Although Zeng *et al.* (2018) recently reported the transcriptome comparing the IRH and the ARB, the expression patterns of genes putatively related to nutrient transfer and metabolism have not been analyzed in detail. AMF extend extraradical structures in order to absorb nutrients from soil and produce spores. Straight thick hyphae called runner hyphae (RH) are spread out from the root (Fig. 1b, c), and subsequently, highly branched hyphae called branched absorbing structures (BAS) differentiate on the RH (Fig. 1b, c) (Bago et al., 1998a). Daughter spores are formed on the BAS, and gradually mature (Fig. 1b, d) (Bago et al., 1998a). The features of each cell type in the extraradical structures, responsible for nutrient absorption and metabolism, are completely unknown. Previous studies speculated that the BAS have important roles for nutrient absorption because of their cytological similarity with ARB and because the pH of the media around the BAS forming spores decreases, presumably by the secretion of compounds for phosphate solubilization (Bago et al., 1998a, 1998b). However, there is no direct evidence to show nutrient absorption by the BAS. Several studies have reported transcriptome analyses comparing the ERM with the IRM or germinating spores (Kikuchi et al., 2014; Tisserant et al., 2013, 2012; Tsuzuki et al., 2016), but to our knowledge, there are no reports that comprehensively investigate the spatial gene expression pattern among the cell types of extraradical structures.

Here, we show the cell type-specific transcriptome of the model AMF species, *Rhizophagus irregularis*. We separated the extraradical structures into five cell types, GT, RH, BAS, immature spores (IS), and mature spores (MS), and performed RNA-seq

bioRxiv preprint doi: https://doi.org/10.1101/491811; this version posted December 11, 2018. The copyright holder for this preprint (which was not certified by peer review) is the author/funder, who has granted bioRxiv a license to display the preprint in perpetuity. It is made available under aCC-BY-NC-ND 4.0 International license.

130 analysis. To overcome the low volume of sample available, we applied the SMART-seq2
131 method, in which we were able to construct RNA-seq libraries from as little as 10 pg of
132 RNA (Picelli et al., 2014, 2013). In addition, we reanalyzed the most recent RNA-seq
133 data comparing ARB and the IRH (Zeng et al., 2018), focusing on the genes possibly
134 involved in nutrient transfer to host plants. Our analyses successfully captured the
135 physiological features of each cell type and revealed cell type-specific expression patterns
136 of genes related to absorption, metabolism, and transfer of nutrients. These results provide
137 a basic dataset to understand nutrient exchange, which is the central function of AM
138 symbiosis.
139
140 **Results**
141 **Cell type-specific transcriptome analysis of *R. irregularis* using the low input RNA-**
142 **seq method**
143 To investigate the physiological features of the extraradical structures of AMF, we
144 performed transcriptome analysis in *R. irregularis* DAOM197198, comparing five cell
145 types of the extraradical structures, GT, RH, BAS, IS, and MS (Fig. 1e–i). As it was
146 difficult to collect sufficient amounts of samples for the regular RNA-seq method, we
147 constructed the RNA-seq libraries using the SMART-seq2 method, a low input library
148 preparation method (Picelli et al., 2014, 2013). The libraries were sequenced using the
149 Illumina HiSeq1500 and the reads obtained were analyzed based on the latest genome
150 data (Supplemental Table S1) (Maeda et al., 2018).
151 We first validated the sampling and sequencing method by using principal component
152 analysis (PCA) of gene expression profiles among cell types and replicates (Fig. 2a). PC1
153 clearly discriminated between hyphae and spores, while PC2 captured the maturation of

bioRxiv preprint doi: https://doi.org/10.1101/491811; this version posted December 11, 2018. The copyright holder for this preprint (which was not certified by peer review) is the author/funder, who has granted bioRxiv a license to display the preprint in perpetuity. It is made available under aCC-BY-NC-ND 4.0 International license.

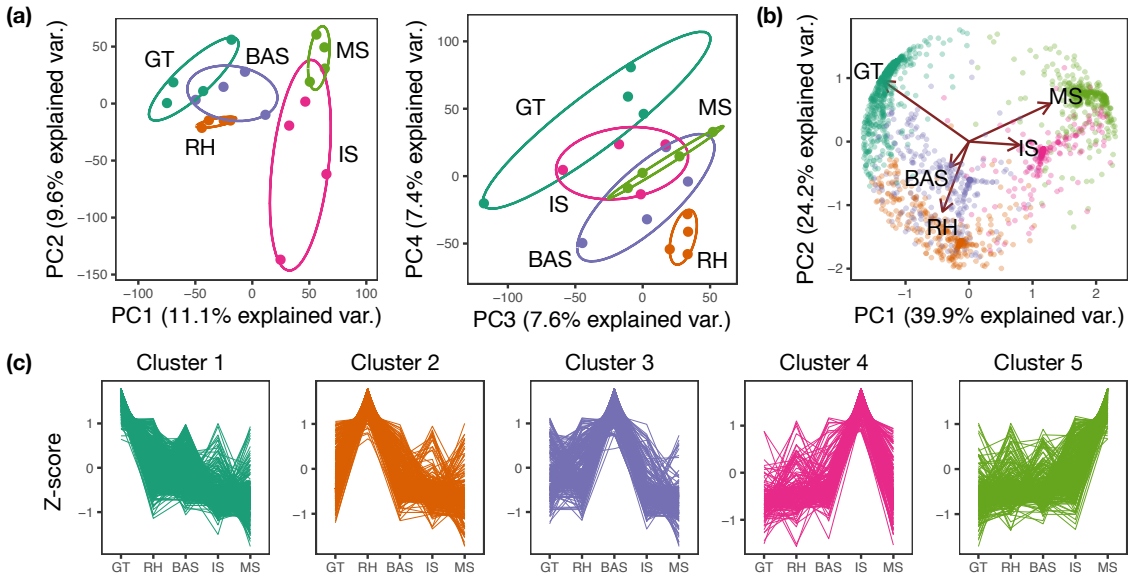

Fig. 2 Detection of cell type-specific gene expression. (a) Principal component analysis (PCA) of gene expression profiles between cell types and replicates. Ellipses represent a 68 % confidence region for each cell type. **(b)** PCA analysis of 1,977 differentially expressed genes (DEGs). DEGs were classified into five clusters using the K-means method. **(c)** The scaled expression levels of genes in each cluster. Genes in the same clusters are labelled in the same color. GT, germ tubes; RH, runner hyphae; BAS, branched absorbing structures; IS, immature spores; MS, mature spores.

spores. Although hyphae samples were not clearly separated in the PC1-PC2 plane, they were separated in the PC3-PC4 plane. These results indicated that the low input RNA-seq method successfully detected the differences in gene expression patterns among cell types.

Among the 19,918 genes expressed in all the samples, 1,977 genes were differentially expressed among cell types (Supplemental Table S2). To visualize the expression pattern of the differentially expressed genes (DEGs), we again performed PCA. The axes of the five cell types indicated that PC1 demonstrates whether the DEGs were expressed in hyphae or spores and that PC2 demonstrates whether they were expressed in pre-symbiotic hyphae, GT, or symbiotic extraradical hyphae, RH and BAS (Fig. 2b). This

bioRxiv preprint doi: https://doi.org/10.1101/491811; this version posted December 11, 2018. The copyright holder for this preprint (which was not certified by peer review) is the author/funder, who has granted bioRxiv a license to display the preprint in perpetuity. It is made available under aCC-BY-NC-ND 4.0 International license.

result seems reasonable considering the functional similarity of the cell types.

DEGs were densely mapped near the axis of each cell type, showing that many DEGs were highly expressed in one cell type only (Fig. 2b). Therefore, we classified the DEGs into five clusters using the K-means method. Clusters 1, 2, 3, 4 and 5 were represented by genes highly expressed in the GT, RH, BAS, IS, or MS, respectively (Fig. 2b, c). To investigate the function of genes in each cluster, we performed gene ontology (GO) enrichment analysis using the GO term Biological Process (Supplemental Table S3). In cluster 3, the GO term 'transmembrane transport' (GO:0055085) was enriched. Although called 'branching absorbing structures', there is no direct evidence to show nutrient absorption by the BAS (Bago et al., 1998a, 1998b). Our result, however, strongly suggests the involvement of the BAS in nutrient absorption. The enrichment of many GO terms involved in DNA replication and nuclear cell division in cluster 4 appears to reflect the burst in mitosis that occurs during spore maturation (Marleau et al., 2011). Thus, the results of the GO enrichment analysis are consistent with previous observations, suggesting that our RNA-seq analysis captured the characteristic transcriptional profiles of each cell type.

Survey of genes related to absorption, metabolism and transfer of nutrients

To date, many studies have identified the genes related to absorption, metabolism, and transfer of nutrients in *R. irregularis*. These genes, however, have been annotated based on past transcriptome or genome data and are sometimes named differently in different reports (e.g., *GiPT* in Maldonado-Mendoza et al., 2001 and *RiPT1* in Walder et al., 2016). Therefore, we re-annotated these genes based on our current genome data (Maeda et al., 2018), and re-named them uniformly, using the reported gene names (Supplemental Table

bioRxiv preprint doi: https://doi.org/10.1101/491811; this version posted December 11, 2018. The copyright holder for this preprint (which was not certified by peer review) is the author/funder, who has granted bioRxiv a license to display the preprint in perpetuity. It is made available under aCC-BY-NC-ND 4.0 International license.

196 S4). In addition, we searched unidentified genes, putatively related to absorption,
197 metabolism, and transfer of nutrients, based on orthology with the genes of
198 *Saccharomyces cerevisiae* or *Aspergillus nidurans*, as detected by the OrthoFinder
199 software (Supplemental Table S4) (Emms and Kelly, 2015; Maeda et al., 2018). Next, we
200 examined the expression patterns of these genes, as discussed below.
201
202 **Absorption and metabolism of mineral nutrients**
203 Two of three genes encoding H^+–Pi co-transporters, *PT1* and *PT2*, were differentially
204 expressed among cell types, while *PT3* and two genes encoding Na^+–Pi co-transporters,
205 *PT5* and *PT6*, were not differentially expressed and showed relatively low expression
206 levels (Fig. 3a, Supplemental Table S4). *PT1* was the most highly expressed gene among
207 the phosphate transporters and showed the highest expression level in the BAS (Fig. 3a).
208 *ACP1*, a gene encoding acid phosphatase, was strongly expressed in the MS (Fig. 3b),
209 which is consistent with a previous observation in which the pH of the media around the
210 BAS containing spores was decreased (Bago et al., 1998b). These results indicate the
211 importance of the BAS for Pi absorption. *VTC1*, which is thought to be involved in Pi
212 polymerization, was significantly highly expressed in the RH, while *PPN3*, a gene
213 encoding endopolyphosphatase, was highly expressed in the BAS, suggesting that Pi
214 metabolism is specifically regulated in the RH and BAS (Fig. 3c,d).
215 The expression of *AMT1* was dominant in extraradical structures among ammonium
216 transporters (Fig. 3e). *AMT1* was expressed at relatively high levels in all cell types
217 examined, especially in the BAS (Fig. 3e). The expression of genes encoding glutamine

bioRxiv preprint doi: https://doi.org/10.1101/491811; this version posted December 11, 2018. The copyright holder for this preprint (which was not certified by peer review) is the author/funder, who has granted bioRxiv a license to display the preprint in perpetuity. It is made available under aCC-BY-NC-ND 4.0 International license.

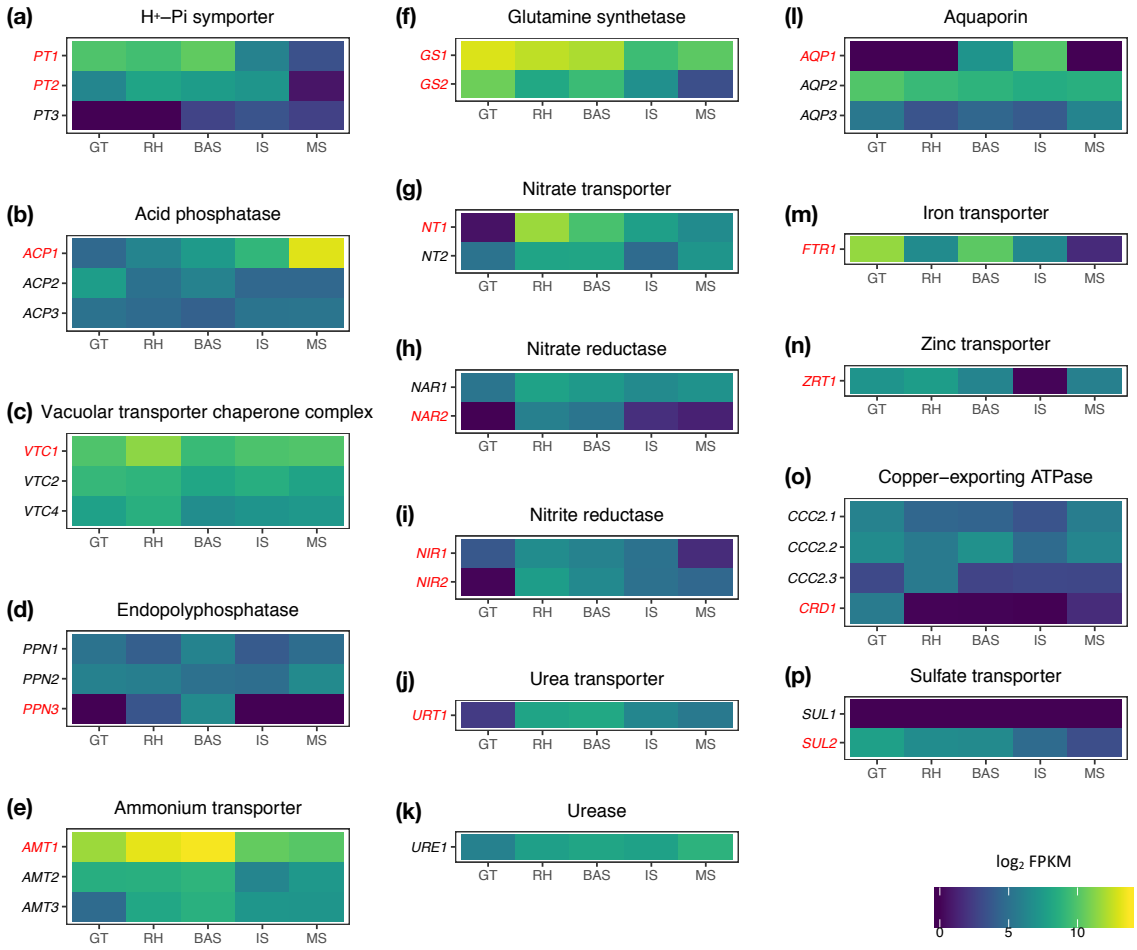

Fig. 3 Expression patterns of genes related to mineral nutrient absorption and metabolism. Log_2 fragments per kilobase of exon per million reads mapped (FPKM) in each cell type of the genes encoding H^+–Pi symporter **(a)**, acid phosphatase **(b)**, vacuolar transporter chaperone complex **(c)**, endophosphatase **(d)**, ammonium transporter **(e)**, glutamine synthase **(f)**, nitrate transporter **(g)**, nitrate reductase **(h)**, nitrite reductase **(i)**, urea transporter **(j)**, urease **(k)**, aquaporin **(l)**, iron transporter **(m)**, zinc transporter **(n)**, copper-exporting ATPase **(o)**, and sulfate transporter **(p)**. The expression of genes in red letters was statistically significantly different among the cell types (FDR < 0.05). GT, germ tubes; RH, runner hyphae; BAS, branched absorbing structures; IS, immature spores; MS, mature spores.

synthase, the first step in ammonium assimilation, was highest in the GT, and in other cell types as well (Fig. 3f). Considering the expression pattern of these genes, AMF may use

bioRxiv preprint doi: https://doi.org/10.1101/491811; this version posted December 11, 2018. The copyright holder for this preprint (which was not certified by peer review) is the author/funder, who has granted bioRxiv a license to display the preprint in perpetuity. It is made available under aCC-BY-NC-ND 4.0 International license.

232 ammonium as a nitrogen source in all life stages. Conversely, genes encoding nitrate
233 transporter, nitrate reductase, and nitrite reductase were highly expressed in the RH while
234 strongly suppressed in the GT (Fig. 3g–i), indicating that the RH has a central role in
235 nitrate metabolism and that *R. irregularis* cannot utilize nitrate in pre-symbiotic stages.
236 As the reduction of nitrate to ammonium requires high energy (Courty et al., 2015), it
237 seems reasonable that the AMF assimilates nitrate in the symbiotic stages only, where
238 they can obtain sufficient carbon sources from host plants. The expression patterns of the
239 genes encoding urea transporter and urease were similar to those of nitrate-related genes
240 (Fig. 3j,k). Some arginine metabolism genes were differentially expressed among cell
241 types, but their expression did not follow a particular pattern (Supplemental Table S4).
242 One of three genes encoding aquaporin, *AQP1*, was expressed specifically in the IS
243 (Fig. 3l). As AQY1, a yeast spore-specific aquaporin, may function in spore maturation
244 (Sidoux-Walter et al., 2004), *AQP1* might also be involved in this process. Genes
245 encoding iron transporter, zinc transporter, copper-exporting ATPase, and sulfate
246 transporter were also differentially expressed among cell types (Fig. 3m–p).
247
248 **Carbon absorption and metabolism**
249 Consistent with the previous observation that AMF can absorb acetate and
250 monosaccharide from the ERM (Helber et al., 2011; Pfeffer et al., 1999), the expression
251 of acetate transporters, carboxylate transporters and monosaccharide transporters was
252 clearly detected in extraradical structures (Fig. 4a–c). As our previous phylogenetic
253 analysis classified *RiMST6* (Ait Lahmidi et al., 2016) as a carboxylate transporter (Maeda
254 et al., 2018), we re-named it *JEN2* (Fig. 4b and Supplemental Table S4). While genes
255 encoding acetate transporter were expressed in a broad range of cell types, the expression

bioRxiv preprint doi: https://doi.org/10.1101/491811; this version posted December 11, 2018. The copyright holder for this preprint (which was not certified by peer review) is the author/funder, who has granted bioRxiv a license to display the preprint in perpetuity. It is made available under aCC-BY-NC-ND 4.0 International license.

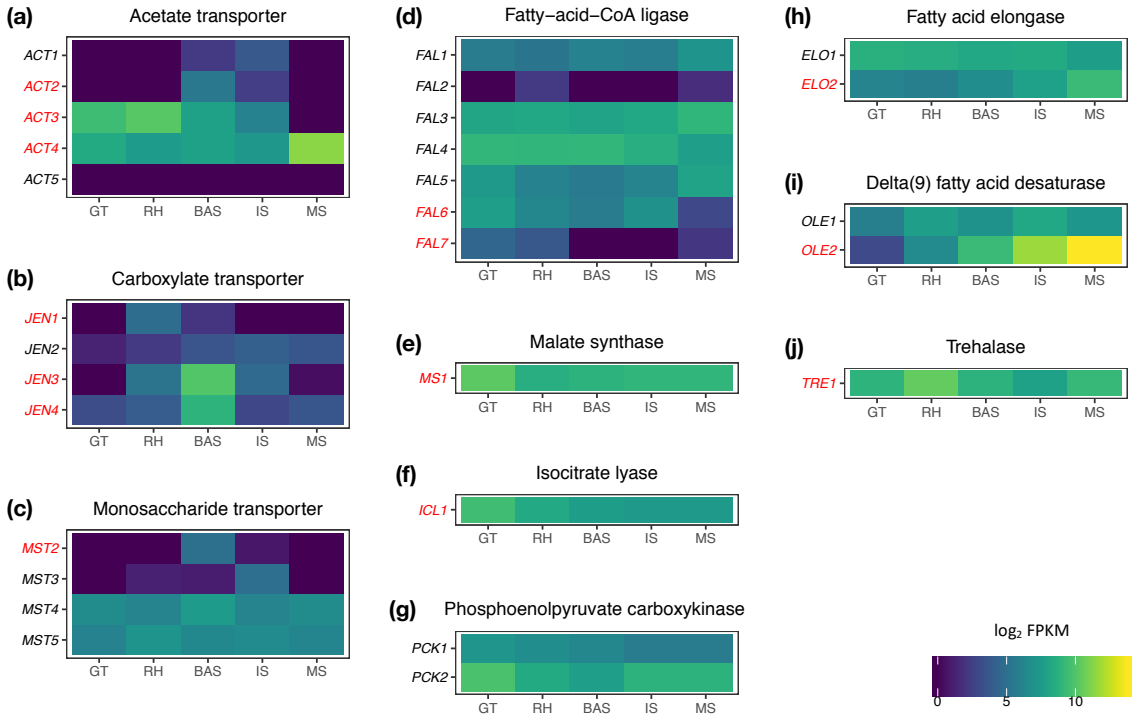

Fig. 4 Expression patterns of genes related to carbon absorption and metabolism. Log_2 fragments per kilobase of exon per million reads mapped (FPKM) in each cell type of the genes encoding acetate transporter **(a)**, carboxylate transporter **(b)**, monosaccharide transporter **(c)**, Fatty-acid-CoA ligase **(d)**, malate synthase **(e)**, isocitrate lyase **(f)**, phosphoenolpyruvate carboxykinase **(g)**, fatty acid elongase **(h)**, delta 9-fatty acid desaturase **(i)**, and trehalase **(j).** The expression of genes in red letters was statistically significantly different among the cell types (FDR < 0.05). GT, germ tubes; RH, runner hyphae; BAS, branched absorbing structures; IS, immature spores; MS, mature spores.

of *JEN3* and *JEN4*, genes encoding carboxylate transporters, were almost BAS-specific (Fig. 4a,b). MST2 is a monosaccharide transporter which is expressed in the IRM and required for mycorrhiza formation involving arbuscule development (Helber et al., 2011). While expression of *MST2* in the ERM was not detected previously (Helber et al., 2011), a relatively low but clear level of expression was observed in the BAS (Fig. 4c). These results indicate that the BAS is also important for carbon source absorption.

Two of seven genes encoding fatty-acid-CoA ligase, which functions in the β-

bioRxiv preprint doi: https://doi.org/10.1101/491811; this version posted December 11, 2018. The copyright holder for this preprint (which was not certified by peer review) is the author/funder, who has granted bioRxiv a license to display the preprint in perpetuity. It is made available under aCC-BY-NC-ND 4.0 International license.

oxidation pathway, were differentially expressed among cell types, and showed the highest expression levels in the GT (Fig. 4d). In addition, both of the genes encoding glyoxylate cycle-specific enzymes, isocitrate lyase and malate synthase, were significantly highly expressed in the GT (Fig. 4e,f). Genes encoding phosphoenolpyruvate carboxykinase, an enzyme functioning in gluconeogenesis, were also highly expressed in the GT, although the differences were not statistically significant (Fig. 4g). These expression patterns are consistent with reports that most of the carbon storage in the spores of AMF is in the form of lipids and fatty acids (Bécard et al., 1991; Jabaji-hare, 1988). Conversely, two genes encoding enzymes for the modification of fatty acids, fatty acid elongase and delta 9-fatty acid desaturase, were highly expressed in the MS (Fig. 4h,i). These genes might have an important contribution to fatty acid storage in spores. On the other hand, the gene encoding trehalase was highly expressed in the RH (Fig. 4j), presumably reflecting the abundant saccharides available from host plants in the symbiotic stages.

Nutrient transfer in arbuscules

To investigate the function of the arbuscule in nutrient exchange between AMF and host plants, we reanalyzed the RNA-seq data comparing the IRH and ARB reported by Zeng et al. (2018). PCA between samples clearly discriminated between the IRH and ARB samples (Fig. 5a).

We then analyzed DEGs between the IRH and ARB. Among the phosphate-related genes examined (Supplemental Table S4), *PPN3*, a gene encoding endophosphatase, and *SYG1-1*, a gene encoding the homolog of a phosphate exporter, were mainly expressed in the ARB compared to the IRH (Fig. 5 b,c). Although the functions of these genes have

bioRxiv preprint doi: https://doi.org/10.1101/491811; this version posted December 11, 2018. The copyright holder for this preprint (which was not certified by peer review) is the author/funder, who has granted bioRxiv a license to display the preprint in perpetuity. It is made available under aCC-BY-NC-ND 4.0 International license.

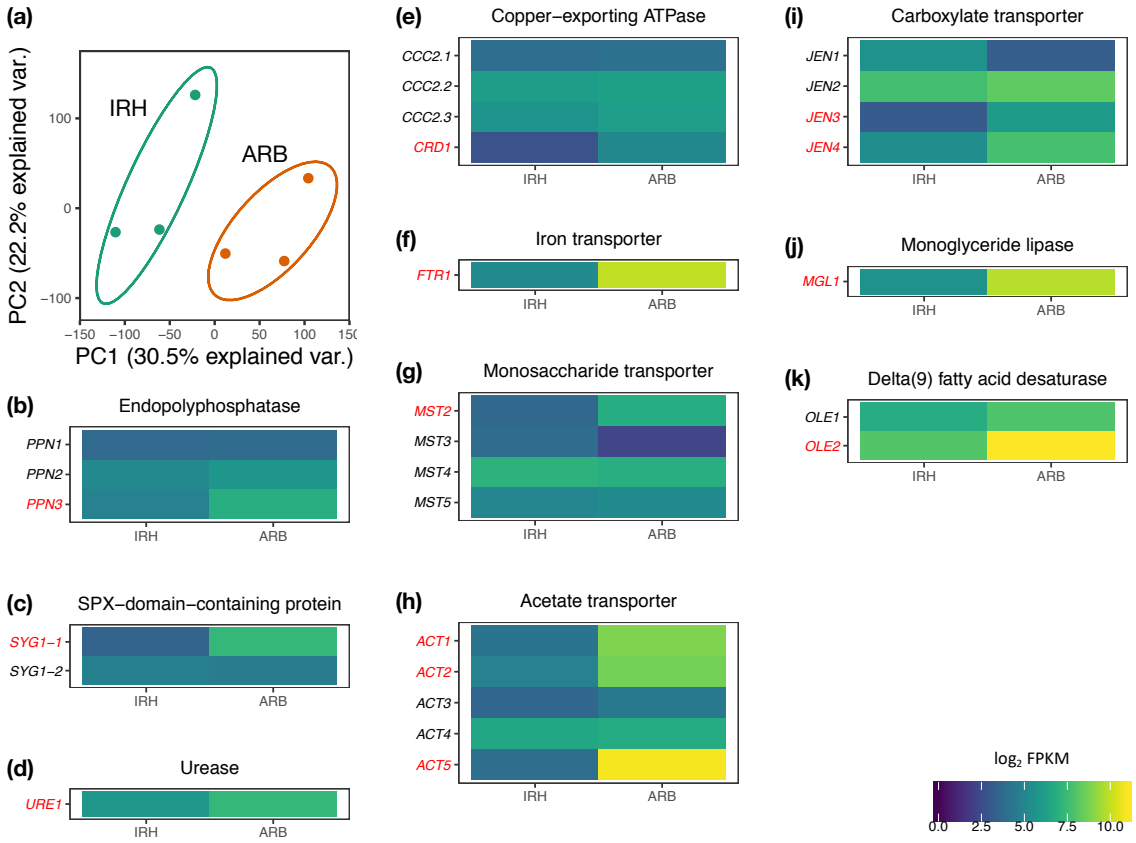

Fig. 5 Differentially expressed genes between intraradical hyphae and arbuscules. **(a)** Principal component analysis (PCA) of gene expression profiles of intraradical hyphae and arbuscule samples. IRH, intraradical hyphae; ARB, arbuscule. **(b–k)** Log_2 fragments per kilobase of exon per million reads mapped (FPKM) in intraradical hyphae or arbuscules of the genes encoding endophosphatase **(b)**, SPX-domain-containing protein **(c)**, urease **(d)**, copper-exporting ATPase **(e)**, iron transporter **(f)**, acetate transporter **(g)**, monosaccharide transporter **(h)**, carboxylate transporter **(i)**, Monoglyceride lipase **(j)**, and delta 9-fatty acid desaturase **(k)**. The expression of genes in red letters was statistically significantly different between the IRH and ARB (FDR < 0.05).

not been investigated, it is possible that they are involved in phosphate release from AMF. In concordance with the report that arginine is degraded into ammonium before nitrogen is transferred to host plants (Jin et al., 2005), urease, which catalyzes the conversion of urea to ammonium in the final step of arginine degradation, was highly expressed in the

bioRxiv preprint doi: https://doi.org/10.1101/491811; this version posted December 11, 2018. The copyright holder for this preprint (which was not certified by peer review) is the author/funder, who has granted bioRxiv a license to display the preprint in perpetuity. It is made available under aCC-BY-NC-ND 4.0 International license.

313 ARB (Fig. 5d). *CRD1*, a gene encoding copper-exporting ATPase, and *FTR1*, a gene
314 encoding an iron transporter, were also highly expressed in the ARB (Fig. 5e,f). Although
315 *MST2* was expressed in both the IRH and ARB, its expression level was higher in the
316 ARB (Fig. 5g), indicating that the ARB has a significant role in saccharide absorption.
317 The expression of some genes encoding acetate transporters and carboxylate transporters
318 was also induced in the ARB (Fig. 5h,i). Two lipid metabolism-related genes *MGL1* and
319 *OLE2*, which encode monoacylglyceride lipase and delta 9-fatty acid desaturase,
320 respectively, were highly expressed in the ARB (Fig. 5j,k). This result led us to
321 hypothesize that *sn*-2-palmitoylglycerol is hydrolyzed into palmitoic acid and glycerol by
322 MGL1, and palmitoic acid is desaturated by OLE2. Thus, analysis of the expression
323 patterns of putative nutrient transfer genes has provided insight into the functions of the
324 ARB for nutrient exchange between AMF and host plants.
325
326 **Discussion**
327 In this study, we performed transcriptome analysis comparing cell types in extraradical
328 structures of the AMF *R. irregularis* to investigate the functions of these cell types in
329 nutrient absorption and metabolism. Our analysis generated cell type-specific
330 transcriptional profiles and detected DEGs among cell types. Further analysis of genes
331 related to nutrient absorption and metabolism, and reannotation using the latest genome
332 data, revealed the characteristic functions of each cell type; for example, fatty acid
333 consumption in the GT (Fig. 4d–g), nitrate absorption and reduction in the RH (Fig. 3f–
334 i), phosphate, ammonium, and carbon source absorption in the BAS (Fig. 3a,e; Fig. 4a–
335 c), and fatty acid modification in the MS (Fig. 4h,i). In addition, we reanalyzed the RNA-
336 seq data comparing the IRH and ARB (Zeng et al., 2018) and detected the expression of

bioRxiv preprint doi: https://doi.org/10.1101/491811; this version posted December 11, 2018. The copyright holder for this preprint (which was not certified by peer review) is the author/funder, who has granted bioRxiv a license to display the preprint in perpetuity. It is made available under aCC-BY-NC-ND 4.0 International license.

337 putative nutrient transfer genes in the ARB (Fig. 5). Although many studies have revealed
338 the regulation of absorption, metabolism, and transfer of nutrients by AMF, the spatial
339 regulations associated with cell differentiation remain largely unknown. Our data,
340 therefore, provides comprehensive information for understanding the dynamics of
341 nutrient regulation in this symbiotic system.

342 Of note, our results suggest distinctive functions between the RH and BAS for
343 nutrient absorption and metabolism. Although they have morphological differences, it
344 was not clear previously as to whether the RH and BAS have different transcriptional
345 profiles, because they are not separated by either a cell membrane nor a cell wall and
346 share a common cytoplasm (Bago et al., 1998a). This question had not been approached
347 previously, probably because of technical difficulties. Our RNA-seq analysis using the
348 SMART-seq2 method clearly illustrated the difference in the transcriptome between the
349 two cell types, indicating the importance of the RH for the absorption and reduction of
350 nitrate (Fig. 3g–i) and that of the BAS for the absorption of phosphate, ammonium,
351 carboxylate, and monosaccharide (Fig. 3a,e; Fig. 4a–c). These results provide a new
352 perspective for investigating nutrient absorption and metabolism in AMF.

353 To further understand the physiological functions of each cell type, functional
354 analysis of DEGs is required. Host-induced gene silencing (HIGS) and virus-induced
355 gene silencing (VIGS), which are able to silence the genes of AMF in the IRM by using
356 dsRNA produced by the host plant or a virus to infect the host plant, respectively, (Helber
357 et al., 2011; Kikuchi et al., 2016; Tsuzuki et al., 2016), will be useful tools for the analysis
358 of the putative nutrient transfer genes expressed in the ARB. However, no method to
359 manipulate gene expression in extraradical structures currently exists. Establishment of
360 new technologies for transformation, gene silencing in extraradical structures and

bioRxiv preprint doi: https://doi.org/10.1101/491811; this version posted December 11, 2018. The copyright holder for this preprint (which was not certified by peer review) is the author/funder, who has granted bioRxiv a license to display the preprint in perpetuity. It is made available under aCC-BY-NC-ND 4.0 International license.

mutagenesis is therefore necessary.

In addition to absorption and metabolism of nutrients, extraradical structures have important functions such as infection in host plants, interaction with associated bacteria, and spore formation, the genetics of which have been poorly investigated. Our data provide fundamental information which should assist in these investigations.

Materials and Methods

Biological materials and growth conditions. Hairy roots of carrot (*Daucus carota*), generated as described in Tsuzuki *et al.* (2016), were grown on M medium (Bécard and Fortin 1988). Monoxenic cultures of the hairy root and *Rhizophagus irregularis* DAOM 197198 (Premier Tech, Rivière-du-Loup, Canada) were performed as described in Tsuzuki *et al.* (2016).

RNA-seq analysis. Germ tubes were sampled from 7 days after inoculation (dai) monoxenic culture plates. The hyphae which did not attach to the hairy root were selected. The other cells were sampled from 42 dai plates. Spores smaller than 100 μM in diameter were defined as immature spores, while the larger ones were defined as mature spores. RNA was extracted using NucleoSpin RNA XS (Macherey-Nagel, Düren, Germany), reverse-transcribed and amplified using the SMART-Seq v4 Ultra Low Input RNA Kit for Sequencing (Clontech, Mountain View, CA, USA) (Picelli et al., 2014, 2013). The quality and the quantity of cDNA was checked using the Agilent 2100 Bioanalyzer with the High Sensitivity DNA kit (Agilent Technologies, Santa Clara, CA, USA). cDNA was sheared using the COVARIS S2 system (Covaris Inc., Woburn, MA, USA) and converted to RNA-seq libraries using the Low input library prep kit (Clontech, Mountain View, CA,

bioRxiv preprint doi: https://doi.org/10.1101/491811; this version posted December 11, 2018. The copyright holder for this preprint (which was not certified by peer review) is the author/funder, who has granted bioRxiv a license to display the preprint in perpetuity. It is made available under aCC-BY-NC-ND 4.0 International license.

385 USA). Four replicates were prepared for each cell type. 102 bp single-end reads were
386 obtained using the HiSeq 1500 (Illumina, San Diego, CA, USA). Raw sequence data has
387 been deposited in the DDBJ Sequence Read Archive (DRA) under BioProject
388 PRJDB6136. The RNA-seq data comparing the IRH and ARB were obtained from
389 BioProject PRJNA389248.

390 These reads were trimmed using Trimmomatic (v0.33) (Bolger et al., 2014). Trimmed
391 reads were mapped to the latest genome data (Maeda et al., 2018) by using tophat2
392 (v2.1.0) (Kim et al., 2013). The read counts were calculated by HT-seq (v0.6.1) (Anders
393 et al., 2015). DEGs ($|\log_2 FC| > 1$, FDR < 0.05) were detected using EdgeR-robust
394 (v3.18.1) (Robinson et al., 2010; Zhou et al., 2014).

395 For PCA, we scaled all TMM normalized CPM (Robinson et al., 2010) using the scale
396 function in R (v3.4.1). PCA was performed using the prcomp function in R, using all
397 expressed genes. For PCA comparing the DEGs, the expression levels of DEGs in each
398 cell type calculated by EdgeR-robust were scaled using the scale function in R and PCA
399 was performed using the prcomp function in R. K-means classification of DEGs was
400 performed using the kmeans function in R.

401

402 **Acknowledgements**

403 We thank Dr. Syusaku Tsuzuki, Dr. Naoya Takeda, Dr. Katsuharu Saito, and Prof.
404 Tatsuhiro Ezawa for their critical suggestions and Ms. Yuko Ogawa, Ms. Sachiko Tanakta,
405 Ms. Asami Tokairin and Ms. Yumi Yoshinori for their experimental support. We
406 appreciate Dr. Katsushi Yamaguchi, Prof. Shuji Shigenobu, Functional Genomics Facility
407 and Data Integration and Analysis Facility, NIBB Core Research Facilities for their
408 technical support. This work was supported by ACCEL (JPMJAC1403) from the Japan

bioRxiv preprint doi: https://doi.org/10.1101/491811; this version posted December 11, 2018. The copyright holder for this preprint (which was not certified by peer review) is the author/funder, who has granted bioRxiv a license to display the preprint in perpetuity. It is made available under aCC-BY-NC-ND 4.0 International license.

Science and Technology Agency.

Competing interests

The authors declare no competing interests.

References

Ait Lahmidi N, Courty PE, Brulé D, Chatagnier O, Arnould C, Doidy J, Berta G, Lingua G, Wipf D, Bonneau L. 2016. Sugar exchanges in arbuscular mycorrhiza: RiMST5 and RiMST6, two novel Rhizophagus irregularis monosaccharide transporters, are involved in both sugar uptake from the soil and from the plant partner. *Plant Physiol Biochem* **107**:354–363. doi:10.1016/j.plaphy.2016.06.023

Anders S, Pyl PT, Huber W. 2015. HTSeq—a Python framework to work with high-throughput sequencing data. *Bioinformatics* **31**:166–169. doi:10.1093/bioinformatics/btu638

Azevedo C, Saiardi A. 2017. Eukaryotic phosphate homeostasis: the inositol pyrophosphate perspective. *Trends Biochem Sci* **42**:219–231. doi:10.1016/j.tibs.2016.10.008

Bago B, Azcón-Aguilar C, Goulet A, Piché Y. 1998a. Branched absorbing structures (BAS): a feature of the extraradical mycelium of symbiotic arbuscular mycorrhizal fungi. *New Phytol* **139**:375–388. doi:10.1046/j.1469-8137.1998.00199.x

Bago B, Azcón-Aguilar C, Piché Y. 1998b. Architecture and developmental dynamics of the external mycelium of the arbuscular mycorrhizal fungus Glomus intraradices grown under monoxenic conditions. *Mycologia* **90**:52–62.

Bago B, Pfeffer PE, Abubaker J, Jun J, Allen JW, Brouillette J, Douds DD, Lammers

bioRxiv preprint doi: https://doi.org/10.1101/491811; this version posted December 11, 2018. The copyright holder for this preprint (which was not certified by peer review) is the author/funder, who has granted bioRxiv a license to display the preprint in perpetuity. It is made available under aCC-BY-NC-ND 4.0 International license.

433 PJ, Shachar-Hill Y. 2003. Carbon export from arbuscular mycorrhizal roots
434 involves the translocation of carbohydrate as well as lipid. *Plant Physiol*
435 **131**:1496–1507. doi:10.1104/pp.102.007765
436 Bago B, Pfeffer PE, Douds Jr. DD, Brouillette J, Bécard G, Shachar-Hill Y. 1999.
437 Carbon metabolism in spores of the arbuscular mycorrhizal fungus Glomus
438 intraradicesas revealed by nuclear magnetic resonance spectroscopy. *Plant Physiol*
439 **121**:263–272. doi:10.1104/pp.121.1.263
440 Bago B, Pfeffer PE, Shachar-Hill Y. 2000. Carbon metabolism and transport in
441 arbuscular mycorrhizas. *Plant Physiol* **124**:949–957. doi:10.1104/pp.124.3.949
442 Bécard G, Doner LW, Rolin DB, DOUDS DD, Pfeffer PE. 1991. Identification and
443 quantification of trehalose in vesicular-arbuscular mycorrhizal fungi by in vivo ^{13C}
444 NMR and HPLC analyses. *New Phytol* **118**:547–552. doi:10.1111/j.1469-
445 8137.1991.tb00994.x
446 Bolger AM, Lohse M, Usadel B. 2014. Trimmomatic: a flexible trimmer for Illumina
447 sequence data. *Bioinformatics* **30**:2114–2120. doi:10.1093/bioinformatics/btu170
448 Brands M, Wewer V, Keymer A, Gutjahr C, Dörmann P. 2018. The *Lotus japonicus*
449 acyl-acyl carrier protein thioesterase FatM is required for mycorrhiza formation
450 and lipid accumulation of *Rhizophagus irregularis*. *Plant J* **95**:219–232.
451 doi:10.1111/tpj.13943
452 Bravo A, Brands M, Wewer V, Dörmann P, Harrison MJ. 2017. Arbuscular
453 mycorrhiza-specific enzymes FatM and RAM2 fine-tune lipid biosynthesis to
454 promote development of arbuscular mycorrhiza. *New Phytol* **214**:1631–1645.
455 doi:10.1111/nph.14533
456 Bravo A, York T, Pumplin N, Mueller LA, Harrison MJ. 2016. Genes conserved for

bioRxiv preprint doi: https://doi.org/10.1101/491811; this version posted December 11, 2018. The copyright holder for this preprint (which was not certified by peer review) is the author/funder, who has granted bioRxiv a license to display the preprint in perpetuity. It is made available under aCC-BY-NC-ND 4.0 International license.

457 arbuscular mycorrhizal symbiosis identified through phylogenomics. *Nat Plants*
458 **2**:15208. doi:10.1038/nplants.2015.208
459 Breuillin-Sessoms F, Floss DS, Gomez SK, Pumplin N, Ding Y, Levesque-Tremblay V,
460 Noar RD, Daniels DA, Bravo A, Eaglesham JB, Benedito VA, Udvardi MK,
461 Harrison MJ. 2015. Suppression of arbuscule degeneration in Medicago truncatula
462 phosphate transporter4 mutants is dependent on the ammonium transporter 2
463 family protein AMT2;3. *Plant Cell* **27**:1352–1366. doi:10.1105/tpc.114.131144
464 Brundrett MC, Tedersoo L. 2018. Evolutionary history of mycorrhizal symbioses and
465 global host plant diversity. *New Phytol* **220**:1108–1115. doi:10.1111/nph.14976
466 Calabrese S, Pérez-Tienda J, Ellerbeck M, Arnould C, Chatagnier O, Boller T, Schüßler
467 A, Brachmann A, Wipf D, Ferrol N, Courty P-E. 2016. GintAMT3 - a low-affinity
468 ammonium transporter of the arbuscular mycorrhizal Rhizophagus irregularis.
469 *Front Plant Sci* **7**:679. doi:10.3389/fpls.2016.00679
470 Capaccio LCM, Callow JA. 1982. The enzymes of polyphosphate metabolism in
471 vesicular–arbuscular mycorrhizas. *New Phytol* **91**:81–91. doi:10.1111/j.1469-
472 8137.1982.tb03294.x
473 Courty PE, Smith P, Koegel S, Redecker D, Wipf D. 2015. Inorganic nitrogen uptake
474 and transport in beneficial plant root-microbe interactions. *CRC Crit Rev Plant Sci*
475 **34**:4–16. doi:10.1080/07352689.2014.897897
476 Cruz C, Egsgaard H, Trujillo C, Ambus P, Requena N, Martins-Loucao MA, Jakobsen
477 I. 2007. Enzymatic evidence for the key role of arginine in nitrogen translocation
478 by arbuscular mycorrhizal fungi. *Plant Physiol* **144**:782–792.
479 doi:10.1104/pp.106.090522
480 Emms DM, Kelly S. 2015. OrthoFinder: solving fundamental biases in whole genome

bioRxiv preprint doi: https://doi.org/10.1101/491811; this version posted December 11, 2018. The copyright holder for this preprint (which was not certified by peer review) is the author/funder, who has granted bioRxiv a license to display the preprint in perpetuity. It is made available under aCC-BY-NC-ND 4.0 International license.

481 comparisons dramatically improves orthogroup inference accuracy. *Genome Biol*
482 **16**:157. doi:10.1186/s13059-015-0721-2
483 Ezawa T, Saito K. 2018. How do arbuscular mycorrhizal fungi handle phosphate? New
484 insight into fine-tuning of phosphate metabolism. *New Phytol* **220**:1116–1121.
485 doi:10.1111/nph.15187
486 Fitter AH. 2006. What is the link between carbon and phosphorus fluxes in arbuscular
487 mycorrhizas? A null hypothesis for symbiotic function. *New Phytol* **172**:3–6.
488 doi:10.1111/j.1469-8137.2006.01865.x
489 Govindarajulu M, Pfeffer PE, Jin H, Abubaker J, Douds DD, Allen JW, Bücking H,
490 Lammers PJ, Shachar-Hill Y. 2005. Nitrogen transfer in the arbuscular mycorrhizal
491 symbiosis. *Nature* **435**:819–823. doi:10.1038/nature03610
492 Harrison MJ, Dewbre GR, Liu JY. 2002. A phosphate transporter from Medicago
493 truncatula involved in the acquisiton of phosphate released by arbuscular
494 mycorrhizal fungi. *Plant Cell* **14**:2413–2429. doi:10.1105/tpc.004861.the
495 Harrison MJ, van Buuren ML. 1995. A phosphate transporter from the mycorrhizal
496 fungus *Glomus versiforme*. *Nature* **378**:626–629. doi:10.1038/378416a0
497 Helber N, Wippel K, Sauer N, Schaarschmidt S, Hause B, Requena N. 2011. A versatile
498 monosaccharide transporter that operates in the arbuscular mycorrhizal fungus
499 *Glomus* sp is crucial for the symbiotic relationship with plants. *Plant Cell*
500 **23**:3812–3823. doi:10.1105/tpc.111.089813
501 Hijikata N, Murase M, Tani C, Ohtomo R, Osaki M, Ezawa T. 2010. Polyphosphate has
502 a central role in the rapid and massive accumulation of phosphorus in extraradical
503 mycelium of an arbuscular mycorrhizal fungus. *New Phytol* **186**:285–289.
504 Igiehon NO, Babalola OO. 2017. Biofertilizers and sustainable agriculture: exploring

bioRxiv preprint doi: https://doi.org/10.1101/491811; this version posted December 11, 2018. The copyright holder for this preprint (which was not certified by peer review) is the author/funder, who has granted bioRxiv a license to display the preprint in perpetuity. It is made available under aCC-BY-NC-ND 4.0 International license.

505 arbuscular mycorrhizal fungi. *Appl Microbiol Biotechnol* **101**:4871–4881.
506 doi:10.1007/s00253-017-8344-z
507 Jabaji-hare S. 1988. Lipid and fatty acid profiles of some vesicular-arbuscular
508 mycorrhizal fungi: contribution to taxonomy. *Mycologia* **80**:622–629.
509 Jiang Y, Wang W, Xie Q, Liu N, Liu L, Wang D, Zhang X, Yang C, Chen X, Tang D,
510 Wang E. 2017. Plants transfer lipids to sustain colonization by mutualistic
511 mycorrhizal and parasitic fungi. *Science (80-)* **356**:1172–1175.
512 doi:10.1126/science.1252826
513 Jin H, Pfeffer PE, Douds DD, Piotrowski E, Lammers PJ, Shachar-Hill Y. 2005. The
514 uptake, metabolism, transport and transfer of nitrogen in an arbuscular mycorrhizal
515 symbiosis. *New Phytol* **168**:687–696. doi:10.1111/j.1469-8137.2005.01536.x
516 Keymer A, Pimprikar P, Wewer V, Huber C, Brands M, Bucerius SL, Delaux PM,
517 Klingl V, von Röpenack-Lahaye E, Wang TL, Eisenreich W, Dörmann P, Parniske
518 M, Gutjahr C. 2017. Lipid transfer from plants to arbuscular mycorrhiza fungi.
519 *Elife* **6**:e29107. doi:10.7554/eLife.29107
520 Kikuchi Y, Hijikata N, Ohtomo R, Handa Y, Kawaguchi M, Saito K, Masuta C, Ezawa
521 T. 2016. Aquaporin-mediated long-distance polyphosphate translocation directed
522 towards the host in arbuscular mycorrhizal symbiosis : application of virus-induced
523 gene silencing. *New Phytol* 1202–1208. doi:10.1111/nph.14016
524 Kikuchi Y, Hijikata N, Yokoyama K, Ohtomo R, Handa Y, Kawaguchi M, Saito K,
525 Ezawa T. 2014. Polyphosphate accumulation is driven by transcriptome alterations
526 that lead to near-synchronous and near-equivalent uptake of inorganic cations in an
527 arbuscular mycorrhizal fungus. *New Phytol* **204**:638–649. doi:10.1111/nph.12937
528 Kim D, Pertea G, Trapnell C, Pimentel H, Kelley R, Salzberg SL. 2013. TopHat2:

bioRxiv preprint doi: https://doi.org/10.1101/491811; this version posted December 11, 2018. The copyright holder for this preprint (which was not certified by peer review) is the author/funder, who has granted bioRxiv a license to display the preprint in perpetuity. It is made available under aCC-BY-NC-ND 4.0 International license.

529 accurate alignment of transcriptomes in the presence of insertions, deletions and
530 gene fusions. *Genome Biol* **14**:R36. doi:10.1186/gb-2013-14-4-r36
531 Kobae Y, Tamura Y, Takai S, Banba M, Hata S. 2010. Localized expression of
532 arbuscular mycorrhiza-inducible ammonium transporters in soybean. *Plant Cell*
533 *Physiol* **51**:1411–1415. doi:10.1093/pcp/pcq099
534 Kobayashi Y, Maeda T, Yamaguchi K, Kameoka H, Tanaka S, Ezawa T, Shigenobu S,
535 Kawaguchi M. 2018. The genome of *Rhizophagus clarus* HR1 reveals a common
536 genetic basis for auxotrophy among arbuscular mycorrhizal fungi. *BMC Genomics*
537 **19**:465. doi:10.1186/s12864-018-4853-0
538 Kuga Y, Saito K, Nayuki K, Peterson RL, Saito M. 2008. Ultrastructure of rapidly
539 frozen and freeze-substituted germ tubes of an arbuscular mycorrhizal fungus and
540 localization of polyphosphate. *New Phytol* **178**:189–200. doi:10.1111/j.1469-
541 8137.2007.02345.x
542 Lammers PJ, Jun J, Abubaker J, Arreola R, Gopalan A, Bago B, Hernandez-Sebastia C,
543 Allen JW, Douds DD, Pfeffer PE, Shachar-Hill Y. 2001. The glyoxylate cycle in
544 an arbuscular mycorrhizal fungus. Carbon flux and gene expression. *Plant Physiol*
545 **127**:1287–1298. doi:10.1104/pp.010375
546 López-Pedrosa A, González-Guerrero M, Valderas A, Azcón-Aguilar C, Ferrol N. 2006.
547 *GintAMT1* encodes a functional high-affinity ammonium transporter that is
548 expressed in the extraradical mycelium of *Glomus intraradices*. *Fungal Genet Biol*
549 **43**:102–110. doi:10.1016/j.fgb.2005.10.005
550 Luginbuehl LH, Menard GN, Kurup S, Van Erp H, Radhakrishnan G V, Breakspear A,
551 Oldroyd GED, Eastmond PJ. 2017. Fatty acids in arbuscular mycorrhizal fungi are
552 synthesized by the host plant. *Science (80-)* **356**:1175–1178.

bioRxiv preprint doi: https://doi.org/10.1101/491811; this version posted December 11, 2018. The copyright holder for this preprint (which was not certified by peer review) is the author/funder, who has granted bioRxiv a license to display the preprint in perpetuity. It is made available under aCC-BY-NC-ND 4.0 International license.

553 doi:10.1038/nrmicro1987

554 Macdonald RM, Lewis M. 1978. The occurrence of some acid phosphatases and
555 dehydrogenases in the vesicular-arbuscular mycorrhizal fungus *Glomus mosseae*.
556 *New Phytol*. doi:10.1111/j.1469-8137.1978.tb02273.x

557 Maeda T, Kobayashi Y, Kameoka H, Okuma N, Takeda N, Yamaguchi K, Bino T,
558 Shigenobu S, Kawaguchi M. 2018. Evidence of non-tandemly repeated rDNAs and
559 their intragenomic heterogeneity in *Rhizophagus irregularis*. *Commun Biol* **1**:87.
560 doi:10.1101/205864

561 Maldonado-Mendoza IE, Dewbre GR, Harrison MJ. 2001. A phosphate transporter gene
562 from the extra-radical mycelium of an arbuscular mycorrhizal fungus *Glomus*
563 *intraradices* is regulated in response to phosphate in the environment. *Mol Plant-*
564 *Microbe Interact* **14**:1140–1148. doi:10.1094/MPMI.2001.14.10.1140

565 Marleau J, Dalpé Y, St-Arnaud M, Hijri M. 2011. Spore development and nuclear
566 inheritance in arbuscular mycorrhizal fungi. *BMC Evol Biol* **11**:51.
567 doi:10.1186/1471-2148-11-51

568 Pearson JN, Jakobsen I. 1993. The relative contribution of hyphae and roots to
569 phosphorus uptake by arbuscular mycorrhizal plants, measured by dual labelling
570 with ^{32}P and ^{33}P. *New Phytol* **124**:489–494. doi:10.1111/j.1469-
571 8137.1993.tb03840.x

572 Pérez-Tienda J, Testillano PS, Balestrini R, Fiorilli V, Azcón-Aguilar C, Ferrol N.
573 2011. GintAMT2, a new member of the ammonium transporter family in the
574 arbuscular mycorrhizal fungus *Glomus intraradices*. *Fungal Genet Biol* **48**:1044–
575 1055. doi:10.1016/j.fgb.2011.08.003

576 Pfeffer PE, Douds Jr DD, Bécard G, Shachar-Hill Y. 1999. Carbon uptake and the

bioRxiv preprint doi: https://doi.org/10.1101/491811; this version posted December 11, 2018. The copyright holder for this preprint (which was not certified by peer review) is the author/funder, who has granted bioRxiv a license to display the preprint in perpetuity. It is made available under aCC-BY-NC-ND 4.0 International license.

577 metabolism and transport of lipids in an arbuscular mycorrhiza. *Plant Physiol*
578 **120**:587–598. doi:10.1104/pp.120.2.587
579 Picelli S, Björklund ÅK, Faridani OR, Sagasser S, Winberg G, Sandberg R. 2013.
580 Smart-seq2 for sensitive full-length transcriptome profiling in single cells. *Nat*
581 *Methods* **10**:1096–1098. doi:10.1038/nmeth.2639
582 Picelli S, Faridani OR, Björklund ÅK, Winberg G, Sagasser S, Sandberg R. 2014. Full-
583 length RNA-seq from single cells using Smart-seq2. *Nat Protoc* **9**:171–181.
584 doi:10.1038/nprot.2014.006
585 Robinson MD, McCarthy DJ, Smyth GK. 2010. edgeR: a Bioconductor package for
586 differential expression analysis of digital gene expression data. *Bioinformatics*
587 **26**:139–140. doi:10.1093/bioinformatics/btp616
588 Roth R, Paszkowski U. 2017. Plant carbon nourishment of arbuscular mycorrhizal
589 fungi. *Curr Opin Plant Biol* **39**:50–56. doi:10.1016/j.pbi.2017.05.008
590 Saito M. 1995. Enzyme activities of the internal hyphae and germinated spores of an
591 arbuscular mycorrhizal fungus, Gigaspora margarita Becker & Hall. *New Phytol*
592 **129**:425–431. doi:10.1111/j.1469-8137.1995.tb04313.x
593 Sato T, Ezawa T, Cheng W, Tawaraya K. 2015. Release of acid phosphatase from
594 extraradical hyphae of arbuscular mycorrhizal fungus *Rhizophagus clarus*. *Soil Sci*
595 *Plant Nutr* **61**:269–274. doi:10.1080/00380768.2014.993298
596 Shachar-Hill Y, Pfeffer PE, Douds D, Osman SF, Doner LW, Ratcliffe RG. 1995.
597 Partitioning of intermediary carbon metabolism in vesicular-arbuscular
598 mycorrhizal leek. *Plant Physiol* **108**:7–15. doi:10.1104/pp.108.1.7
599 Sidoux-Walter F, Pettersson N, Hohmann S. 2004. The *Saccharomyces cerevisiae*
600 aquaporin Aqy1 is involved in sporulation. *Proc Natl Acad Sci U S A* **101**:17422–

bioRxiv preprint doi: https://doi.org/10.1101/491811; this version posted December 11, 2018. The copyright holder for this preprint (which was not certified by peer review) is the author/funder, who has granted bioRxiv a license to display the preprint in perpetuity. It is made available under aCC-BY-NC-ND 4.0 International license.

601 71427. doi:10.1073/pnas.0404337101

602 Sun X, Chen W, Ivanov S, Maclean AM, Wight H, Ramaraj T, Mudge J, Harrison MJ,
603 Fei Z, Harrison MJ. 2018. Genome and evolution of the arbuscular mycorrhizal
604 fungus Diversispora epigaea (formerly Glomus versiforme) and its bacterial
605 endosymbionts. *New Phytol*. doi:10.1111/nph.15472

606 Tang N, San Clemente H, Roy S, Bécard G, Zhao B, Roux C. 2016. A Survey of the
607 gene repertoire of Gigaspora rosea unravels conserved features among
608 glomeromycota for obligate biotrophy. *Front Microbiol* **7**:1–16.
609 doi:10.3389/fmicb.2016.00233

610 Tani C, Ohtomo R, Osaki M, Kuga Y, Ezawa T. 2009. ATP-dependent but proton
611 gradient-independent polyphosphate-synthesizing activity in extraradical hyphae of
612 an arbuscular mycorrhizal fungus. *Appl Environ Microbiol* **75**:7044–7050.
613 doi:10.1128/AEM.01519-09

614 Tian C, Kasiborski B, Koul R, Lammers PJ, Bucking H, Shachar-Hill Y. 2010.
615 Regulation of the nitrogen transfer pathway in the arbuscular mycorrhizal
616 symbiosis: gene characterization and the coordination of expression with nitrogen
617 flux. *Plant Physiol* **153**:1175–1187. doi:10.1104/pp.110.156430

618 Tisserant E, Kohler A, Dozolme-Seddas P, Balestrini R, Benabdellah K, Colard A,
619 Croll D, da Silva C, Gomez SK, Koul R, Ferrol N, Fiorilli V, Formey D, Franken
620 PH, Helber N, Hijri M, Lanfranco L, Lindquist E, Liu Y, Malbreil M, Morin E,
621 Poulain J, Shapiro H, van Tuinen D, Waschke A, Azcón-Aguilar C, Bécard G,
622 Bonfante P, Harrison MJ, Küster H, Lammers P, Paszkowski U, Requena N,
623 Rensing S a., Roux C, Sanders IR, Shachar-Hill Y, Tuskan G, Young JPW,
624 Gianinazzi-Pearson V, Martin F. 2012. The transcriptome of the arbuscular

bioRxiv preprint doi: https://doi.org/10.1101/491811; this version posted December 11, 2018. The copyright holder for this preprint (which was not certified by peer review) is the author/funder, who has granted bioRxiv a license to display the preprint in perpetuity. It is made available under aCC-BY-NC-ND 4.0 International license.

625 mycorrhizal fungus *Glomus intraradices* (DAOM 197198) reveals functional
626 tradeoffs in an obligate symbiont. *New Phytol* **193**:755–769. doi:10.1111/j.1469-
627 8137.2011.03948.x
628 Tisserant E, Malbreil M, Kuo A, Kohler A, Symeonidi A, Balestrini R, Charron P,
629 Duensing N, Frei dit Frey N, Gianinazzi-Pearson V, Gilbert LB, Handa Y, Herr JR,
630 Hijri M, Koul R, Kawaguchi M, Krajinski F, Lammers PJ, Masclaux FG, Murat C,
631 Morin E, Ndikumana S, Pagni M, Petitpierre D, Requena N, Rosikiewicz P, Riley
632 R, Saito K, San Clemente H, Shapiro H, van Tuinen D, Bécard G, Bonfante P,
633 Paszkowski U, Shachar-Hill YY, Tuskan G a, Young JPW, Young PW, Sanders
634 IR, Henrissat B, Rensing S a, Grigoriev I V, Corradi N, Roux C, Martin F. 2013.
635 Genome of an arbuscular mycorrhizal fungus provides insight into the oldest plant
636 symbiosis. *Proc Natl Acad Sci U S A* **110**:20117–20122.
637 doi:10.1073/pnas.1313452110
638 Trépanier M, Bécard G, Moutoglis P, Willemot C, Gagné S, Avis TJ, Rioux J. 2005.
639 Dependence of arbuscular-mycorrhizal fungi on their plant host for palmitic acid
640 synthesis. *Appl Environ Microbiol* **71**:5341–5347. doi:10.1128/AEM.71.9.5341
641 Tsuzuki S, Handa Y, Takeda N, Kawaguchi M. 2016. Strigolactone-induced putative
642 secreted protein 1 is required for the establishment of symbiosis by the arbuscular
643 mycorrhizal fungus *Rhizophagus irregularis*. *Mol Plant-Microbe Interact* **29**:277–
644 286. doi:10.1094/MPMI-10-15-0234-R
645 van der Heijden MGA, Bardgett RD, van Straalen NM. 2008. The unseen majority : soil
646 microbes as drivers of plant diversity and productivity in terrestrial ecosystems.
647 *Ecol Lett* **11**:296–310. doi:10.1111/j.1461-0248.2007.01139.x
648 van der Heijden MGA, John N. Klironomos, Ursic M, Moutoglis P, Streitwolf-Engel R,

bioRxiv preprint doi: https://doi.org/10.1101/491811; this version posted December 11, 2018. The copyright holder for this preprint (which was not certified by peer review) is the author/funder, who has granted bioRxiv a license to display the preprint in perpetuity. It is made available under aCC-BY-NC-ND 4.0 International license.

649 Boller T, Wiemken A, Sanders IR. 1998. Mycorrhizal fungal diversity determines
650 plant biodiversity, ecosystem variability and productivity. *Nature* **396**:69–72.
651 Viereck N, Hansen PE, Jakobsen I. 2004. Phosphate pool dynamics in the arbuscular
652 mycorrhizal fungus *Glomus intraradices* studied by *in vivo* ^{31}P NMR spectroscopy.
653 *New Phytol* **162**:783–794. doi:10.1111/j.1469-8137.2004.01048.x
654 Walder F, Boller T, Wiemken A, Courty PE. 2016. Regulation of plants' phosphate
655 uptake in common mycorrhizal networks: Role of intraradical fungal phosphate
656 transporters. *Plant Signal Behav* **11**:e1131372.
657 doi:10.1080/15592324.2015.1131372
658 Wewer V, Brands M, Dörmann P. 2014. Fatty acid synthesis and lipid metabolism in
659 the obligate biotrophic fungus Rhizophagus irregularis during mycorrhization of
660 Lotus japonicus. *Plant J* **79**:398–412. doi:10.1111/tpj.12566
661 Yang S-Y, Grønlund M, Jakobsen I, Grotemeyer MS, Rentsch D, Miyao A, Hirochika
662 H, Kumar CS, Sundaresan V, Salamin N, Catausan S, Mattes N, Heuer S,
663 Paszkowski U. 2012. Nonredundant regulation of rice arbuscular mycorrhizal
664 symbiosis by two members of the PHOSPHATE TRANSPORTER1 gene family.
665 *Plant Cell* **24**:4236–4251. doi:10.1105/tpc.112.104901
666 Zeng T, Holmer R, Hontelez J, te Lintel-Hekkert B, Marufu L, de Zeeuw T, Wu F,
667 Schijlen E, Bisseling T, Limpens E. 2018. Host- and stage-dependent secretome of
668 the arbuscular mycorrhizal fungus *Rhizophagus irregularis*. *Plant J* 411–425.
669 doi:10.1111/tpj.13908
670 Zhou X, Lindsay H, Robinson MD. 2014. Robustly detecting differential expression in
671 RNA sequencing data using observation weights. *Nucleic Acids Res* **42**:e91.
672 doi:10.1093/nar/gku310

bioRxiv preprint doi: https://doi.org/10.1101/491811; this version posted December 11, 2018. The copyright holder for this preprint (which was not certified by peer review) is the author/funder, who has granted bioRxiv a license to display the preprint in perpetuity. It is made available under aCC-BY-NC-ND 4.0 International license.

673